



Asymmetrical wakes over anisotropic bathymetries

Léo-Paul Euvé, Agnès Maurel, Philippe Petitjeans, Vincent Pagneux

► To cite this version:

Léo-Paul Euvé, Agnès Maurel, Philippe Petitjeans, Vincent Pagneux. Asymmetrical wakes over anisotropic bathymetries. *Journal of Fluid Mechanics*, 2024, 984, pp.R6. <10.1017/jfm.2024.221>. <hal-04780247>

HAL Id: hal-04780247

<https://hal.science/hal-04780247v1>

Submitted on 13 Nov 2024

HAL is a multi-disciplinary open access archive for the deposit and dissemination of scientific research documents, whether they are published or not. The documents may come from teaching and research institutions in France or abroad, or from public or private research centers.

L'archive ouverte pluridisciplinaire **HAL**, est destinée au dépôt et à la diffusion de documents scientifiques de niveau recherche, publiés ou non, émanant des établissements d'enseignement et de recherche français ou étrangers, des laboratoires publics ou privés.



HAL Authorization

Asymmetrical wakes over anisotropic bathymetries

Leo-Paul Euvé^{1†}, Agnès Maurel², Philippe Petitjeans¹, Vincent Pagneux³.

¹PMMH, ESPCI-PSL Univ., CNRS, Sorbonne Univ., Paris Cité Univ., 7 quai St Bernard, 75005 Paris, France

²Institut Langevin, ESPCI-PSL Univ., CNRS, Paris Cité Univ., 1 rue Jussieu, 75005 Paris, France

³LAUM, CNRS, Univ. du Mans, Av. O. Messiaen, 72085 Le Mans, France

(Received xx; revised xx; accepted xx)

The study investigates the impact of a stratified bathymetry, composed of submerged vertical plates, on a ship wake through both theoretical analysis and experimental realization. For sub-wavelength distances between the plates, the analysis relies on a homogenized model that provides an effective, anisotropic, dispersion relation for the propagation of water waves. Our findings reveal that a highly asymmetric wake can be achieved, with the degree of asymmetry contingent upon the ship propagation direction in relation to the plate orientation. This anisotropy is characterized with respect to water depth and to ship length using the dimensionless depth and hull Froude numbers. Laboratory experiments align closely with theoretical predictions, confirming that the asymmetry of the wake can indeed be managed through manipulation of bathymetric conditions.

Key words: Water waves, Ship wake, Metamaterial, Stratified bathymetry.

1. Introduction

Ship wakes can significantly impact coastlines, river banks, and interactions between ships. Understanding and controlling these wakes can be a great asset for preventing bank erosion and reducing ship energy consumption, as wave resistance plays a substantial role in a ship motion resistance (Havelock 1909). Despite a century and a half of study in this specific domain of water waves, with notable contributions from Lord Kelvin Thomson (1887), recent research has challenged the traditional notion of a constant wake angle of 19.47° , particularly for high hull Froude numbers ($\text{Fr}^L = U/\sqrt{gL}$, where L is the ship hull length, U the ship velocity and g the gravitational constant) in both infinite depth (Rabaud & Moisy 2013; Moisy & Rabaud 2014; Noblesse *et al.* 2014; Pethiyagoda *et al.* 2014; Darmon *et al.* 2014) and finite depth scenarios (Fang *et al.* 2011; Pethiyagoda *et al.* 2015; Caplier *et al.* 2016, 2020). In the latter case, the apparent angle is also influenced by the depth Froude number ($\text{Fr}^h = U/\sqrt{gh}$, where h is the water depth).

The shape of wakes can be manipulated through various means, such as analog systems. An example is the study by Luo *et al.* (2003), which explores a diverse and intriguing behavior of Cerenkov radiation in a photonic crystal. The control can be also provided

† Email address for correspondence: leo-paul.euve@espci.fr

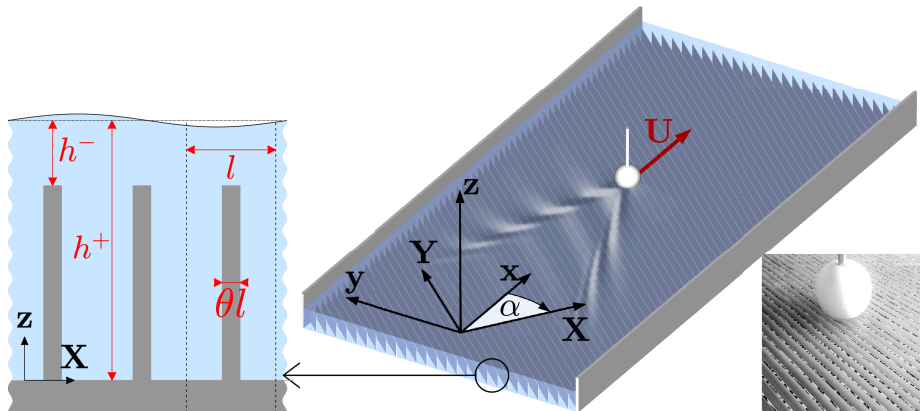


FIGURE 1. Experimental setup with the metamaterial formed by the subwavelength stratified bathymetry. The surface of the metamaterial is around $1.5 \times 1\text{m}^2$ and the region of measurement is $0.7 \times 0.7\text{m}^2$. Parameters : $h^- = 10\text{mm}$, $h^+ = 55\text{mm}$, $l = 12\text{mm}$ and $\theta l = 2\text{mm}$. Top left : geometry of the stratified bathymetry. Center : sketch of the experiment. Bottom right : picture of the plates and the ship (ball).

by applying a specific current, as in Ellingsen (2014) and Li & Ellingsen (2016) where a theory is presented for asymmetric ship wakes in the presence of a shear current with uniform vorticity. In our case, we demonstrate that a ship propagating in an anisotropic metamaterial made of stratified bathymetry can generate highly asymmetric wakes due to the ability of metamaterials to strongly modify wave propagation.

In the following results, the anisotropic metamaterial on the sea bottom is realized using a stratified bathymetry made of submerged vertical plates (figure 1). We begin by characterizing the wake based on the dispersion relation, as proposed in Luo *et al.* (2003) and Carusotto & Rousseaux (2013). Extending this method to the case of anisotropic dispersion (obtained through homogenization), we highlight a wake asymmetry studied in relation to the ship advance direction and speed. Ultimately, the predictive power of this analysis is demonstrated through quantitative results in laboratory experiments.

2. Schematic representation of wakes

In this section, we present the method we use to generate a wake based on the dispersion relation of the medium in which the waves propagate. We start with constant bathymetry to generate known wakes. We then use the dispersion relation of our anisotropic medium to see how it influences the wake and makes it asymmetric.

2.1. Flat bathymetry

To begin with, as a reminder, we consider a flat bathymetry and the classical dispersion relation of water waves (with surface tension due to the scale of the experiment):

$$\omega^2(k) = \left(gk + \frac{\gamma}{\rho} k^3 \right) \tanh(kh), \quad (2.1)$$

with ω the angular frequency, $k = |\mathbf{k}|$ the wavenumber, \mathbf{k} the wavevector, h the water depth, g the gravitational acceleration (9.81m/s^2), γ the surface tension ($72 \cdot 10^{-3}\text{N/m}$ at 25°C) and ρ the water density (1000kg/m^3).

Since the wake is defined as the stationary waves in the referential of the ship, we

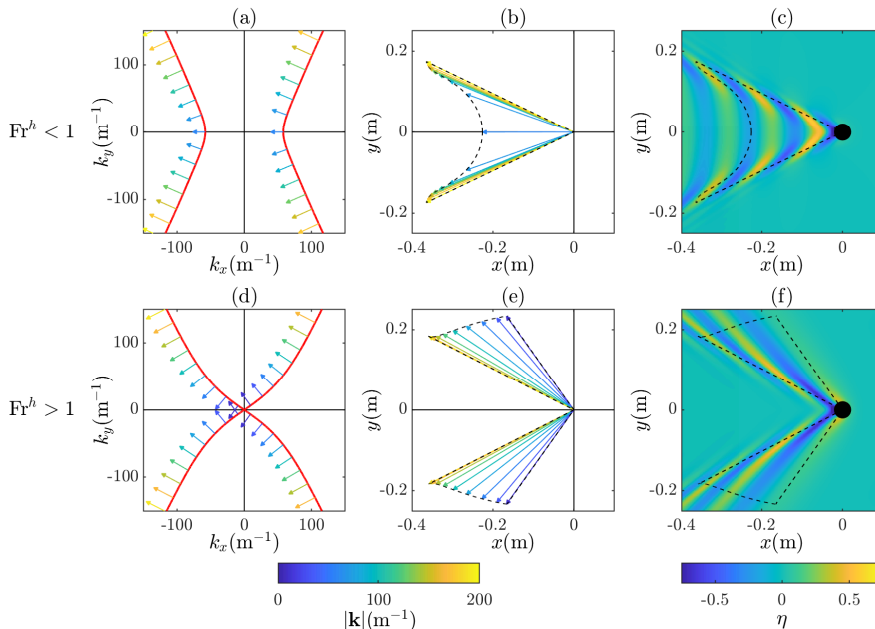


FIGURE 2. (a,d) Classical dispersion relation of wakes (eqs (2.1) and (2.2), red curve). Arrows, normal to the dispersion relation, indicate the group velocity vectors. Their colors indicate the norm of the wavenumber, colorbar. (b,e) Schematic representation of the wake using the group velocity vectors. (c,f) Numerical results for the two wakes. Parameters : $U = 0.415\text{ms}^{-1}$ and $h = 47.5\text{mm}$, $Fr^h = 0.62$ (a,b,c) and $h = 12\text{mm}$, $Fr^h = 1.22$ (d,e,f)

obtain the dispersion relation of the wake through

$$\Omega(\mathbf{k}) = \omega(\mathbf{k}) - \mathbf{U} \cdot \mathbf{k} = 0, \quad (2.2)$$

with Ω the frequency in the ship referential and \mathbf{U} the ship speed vector.

The dispersion relation of the wake, given by the $\mathbf{k} = (k_x, k_y)$ solution of equation (2.2) for a given velocity \mathbf{U} , is shown in figure 2 (a,d) for different water depths corresponding to different depth Froude numbers Fr^h . We also display the group velocity vectors $\mathbf{c}_g = \partial\Omega(\mathbf{k})/\partial\mathbf{k}$ showing the propagation direction of each wavenumbers along the dispersion relation of the wake. As done in Luo *et al.* (2003) and Carusotto & Rousseaux (2013), we can construct a schematic representation of the wake by placing these group velocity vectors in the real space (figure 2(b,e)). This allows us to know the propagation direction of each wavenumber and where the wake energy will be concentrated. These informations simply provided by the dispersion relation are complemented by numerical computation obtained by Fourier transform assuming a Hull Froude number $Fr^L=0.67$ (figure 2(c,f), see Appendix A for the numerical computation). We can recognize the Kelvin wake (Thomson 1887) corresponding to a low Froude number depth (figure 2(c)) and a wake in finite depth (Fang *et al.* 2011; Pethiyagoda *et al.* 2015; Caplier *et al.* 2016, 2020), above the critical $Fr_c^h = 1$, beginning to display Mach cone behaviour (figure 2(f)). Note that, in both cases, we use a Hull Froude number $Fr^L = 0.67$ because it corresponds to the experimental measurements to come.

2.2. Stratified bathymetry

A stratified bathymetry as the one described in figure 1 can be modeled as an effective anisotropic 2D medium when the wave has a wavelength much larger than the period of

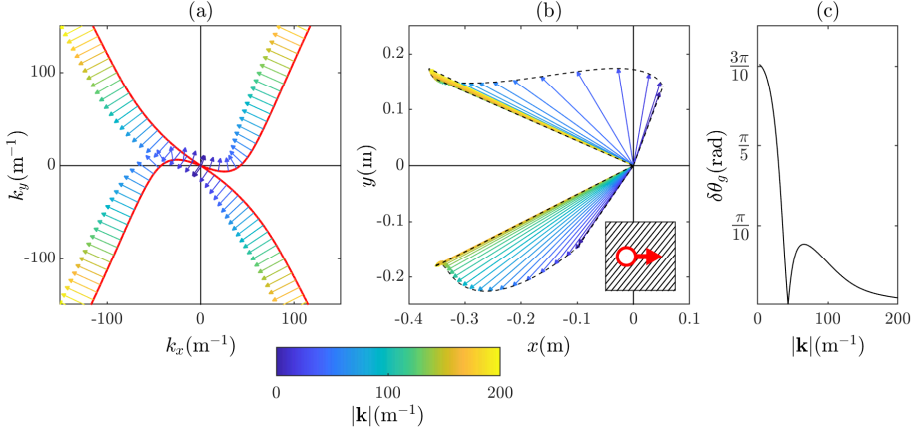


FIGURE 3. (a) Anisotropic dispersion relation (eq. (2.3) and (2.2), red curve) of an asymmetrical wake with $U = 0.415\text{ms}^{-1}$, $h_- = 12\text{mm}$ and $h_+ = 47.5\text{mm}$. The color of each arrow indicates the norm of the wavenumber, colorbar. (b) Schematic representation of the wake using the group velocity vectors, the inset shows the stratified bathymetry with the red arrow indicating the ship propagation. (c) Angle difference, between the upper and lower wake, of the group velocity vector $\delta\theta_g$.

the bathymetry. The two principal axes of this anisotropic medium are \mathbf{X} perpendicular to the plates and \mathbf{Y} parallel to the plates. Unsurprisingly, the angle α between the axis \mathbf{X} and the ship velocity \mathbf{U} is going to be an important parameter to produce the asymmetry of the wake. The dispersion relation over the stratified bathymetry was obtained in Maurel *et al.* (2017) using homogenization techniques:

$$\omega^2(\mathbf{K}) = \left(g \frac{{}^t\mathbf{K} \cdot \mathbf{h} \cdot \mathbf{K}}{\sqrt{{}^t\mathbf{K} \cdot \mathbf{h}^2 \cdot \mathbf{K}}} + \frac{\gamma}{\rho} |\mathbf{K}|^3 \right) \tanh \left(\sqrt{{}^t\mathbf{K} \cdot \mathbf{h}^2 \cdot \mathbf{K}} \right) \quad \text{with} \quad \mathbf{h} = \begin{pmatrix} h_X & 0 \\ 0 & h_Y \end{pmatrix}, \quad (2.3)$$

where \mathbf{K} is the wavevector in the basis (\mathbf{X}, \mathbf{Y}) , $\mathbf{K} = {}^tR_\alpha \mathbf{k}$ the rotation between the two basis (R_α conventional rotation matrix). The anisotropic effective parameters (effective water depths h_X, h_Y) of the structure are obtained using the homogenization of the 3D water wave problem developed in Maurel *et al.* (2017). In (2.3), we added the surface tension effect, considering that the varying bathymetry has no effect on capillary waves.

In the experiments to come, the geometrical parameters of the stratified bathymetry, shown in the figure 1, are set to : $h^- = 10\text{mm}$, $h^+ = 55\text{mm}$, $l = 12\text{mm}$, $\theta = 1/6$ and $l/h^+ = 0.22$. These parameters have been chosen in order to have the most anisotropic medium while avoiding too small water depths susceptible to ignite strong non-linear effects. The homogenization of this setup gives the effective depths $h_X = 12\text{mm}$ and $h_Y = 47.5\text{mm}$. Because the plates are thin ($\theta = 1/6$) and the length of the periodicity is small in front of the highest water depth ($l/h_+ = 0.22$), h_X and h_Y are respectively close to h^- and h^+ (Maurel *et al.* 2017; Marangos & Porter 2021). The anisotropic dispersion relation of the wake (using (2.3) in (2.2) for the parameters $U = 0.415\text{ms}^{-1}$ and $\alpha = 39^\circ$) is shown in figure 3(a). The asymmetry of the dispersion relation between the upper half plane ($k_y > 0$) and the lower half plane ($k_y < 0$) is clearly visible and implies the asymmetry of the wake in the real space as exhibited in figure 3(b). The “lower wake” ($y < 0$) seems to be similar to a wake with a Froude number over one (figure 3(b) compared to figure 2(e)). Quite remarkably, the “upper wake” ($y > 0$) is more peculiar, long waves are ahead of the ship ($x > 0$). In contrast, short waves propagate similarly in both the upper and lower wakes as anticipated from the behaviour of the

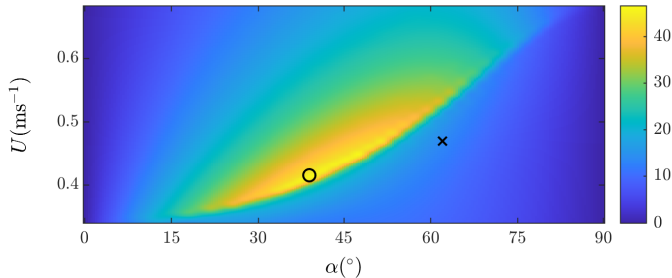


FIGURE 4. Integral of the angle difference for the group velocity vector I_g as a function of the ship velocity U and the angle between the ship and the bathymetry α . The circle corresponds to the parameters used in figure 3. In the following experiments, both the circle and the cross parameters will be chosen.

dispersion relation at large k observed in figure 3(a). This is simply due to the fact that the bathymetry does not affect short waves that are in the deep water regime. Overall, in figure 3(b), the pattern of the wake looks similar to those obtained in Ellingsen (2014) because our bathymetry has an effect that increases with wavelength, as in Ellingsen (2014) where the shear current is a Couette flow with increasing velocity with depth.

To quantify the asymmetry of the wake, we proceed as follows. First, we define $\theta_g(\mathbf{k})$ the angle between the group velocity vector and the horizontal axis in figure 3(b). Then, we can compare the upper and the lower wakes for a given wavenumber with $\delta\theta_g(k) = |\theta_g(y > 0)| - |\theta_g(y < 0)|$ (figure 3(c)). As mentioned previously, long waves are the most impacted by the bathymetry. Next, we use $I_g(\alpha, U) = \int_0^\infty \delta\theta_g(k) dk$ to quantify the global asymmetry of the wake. This quantity is displayed in figure 4 when we vary the ship velocity U and the angle between the ship and the bathymetry α . Note that, the example shown in figure 3 is closed to the maximum asymmetry I_g and the same parameters will be used for the first experiment. Although less asymmetric according to I_g , a second experiment will be performed with another pair of parameters (U , α) exhibiting a different type of asymmetry.

3. Experimental setup

In the experiment, the surface of the metamaterial ($1.5 \times 1\text{m}^2$) is large enough to be considered as an open field and the measurement domain ($0.7 \times 0.7\text{m}^2$) is placed at the end of the varying bathymetry (see figure 1) to observe an established wake. The ship is a ball with a diameter of 80mm (figure 1), this ball is fixed to a guided bar tracked by a motor which provides a constant ship velocity. The ball is submerged by 5mm of water, so the diameter of the surface in contact with the water is 40mm, this dimension is considered as the size of the ship.

We measure the wave field using the optical method called free-surface synthetic Schlieren (FS-SS) based on the analysis of the refracted image of a random dot pattern placed below the free surface (Moisy *et al.* 2009). Since we do not have a flat bottom (due to the varying bathymetry), we paint black dots on the top of the plates to obtain a reference flat surface for the FS-SS method (figure 1 bottom right). We capture 170 images of the surface deformation with an acquisition frequency of 250Hz over the measurement domain $0.7 \times 0.7\text{m}^2$ and then we average the results following the ship (fixing the position of the ship at $(x, y) = (0, 0)$) to suppress the noise coming from some non-stationary waves and the one produced by the measurement method.

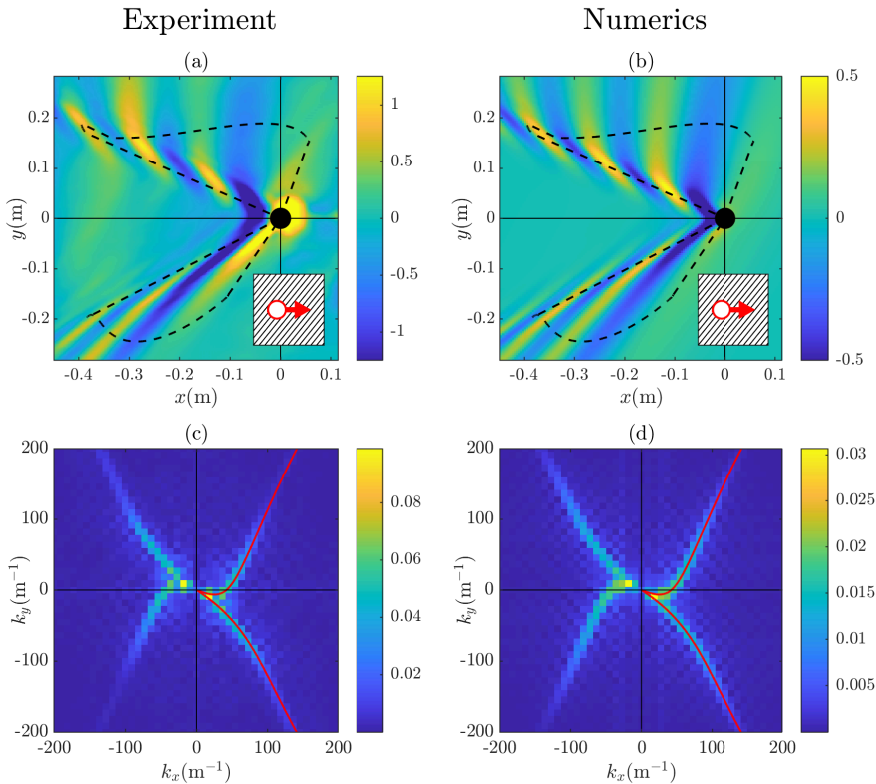


FIGURE 5. Surface elevation for the parameters $h^- = 10\text{mm}$, $h^+ = 55\text{mm}$, $h_X = 12\text{mm}$, $h_Y = 47.5\text{mm}$, $\alpha = -39^\circ$ and $U = 0.415\text{ms}^{-1}$. (a) Experimental results (colorscale in mm), the black dashed line indicated the schematic representation using the group velocity vectors (fig 3b), the inset shows the stratified bathymetry with the red arrow indicating the ship propagation. (c) Fourier transform of the experimental results, the red curve corresponds to the theoretical dispersion relation (2.2) and (2.3). (b) Numerical results (colorscale divided by the maximum value) and (d) its Fourier transform.

4. Experimental Results

For the first experimental results, we consider the same configuration as the theoretical study of figure 3 with the stratified bathymetry $h^- = 10\text{mm}$ and $h^+ = 55\text{mm}$ (effective water depths $h_X = 12\text{mm}$, $h_Y = 47.5\text{mm}$), an angle $\alpha = -39^\circ$ and a ship speed set to $U = 0.415\text{m/s}$ (circle in figure 4). The Froude number based on the depth varies between $\text{Fr}^h = 0.62$ and $\text{Fr}^h = 1.22$ and the hull Froude number is $\text{Fr}^L \simeq 0.7$.

Overall, the measured wake (figure 5(a)) is clearly asymmetric between the upper wake ($y > 0$) and the lower wake ($y < 0$), with even part of long waves ahead of the ship. This experimental result is in good agreement with the schematic representation of the wake using the group velocity (figure 3(b)). The lower wake is the same as the one over a flat bathymetry and a small constant water depth $h = h_X$ (figure 2(f)). The upper wake is the most interesting: on the one hand, the shortest waves are concentrated along the apparent angle which is defined as the angle with the maximum amplitude, but, on the other hand, we can observe long waves far from this angle. Part of those long waves are even ahead of the ship, showing that, in such configuration, some waves have a group velocity higher than the ship speed. We focus on this point in section 5 where is

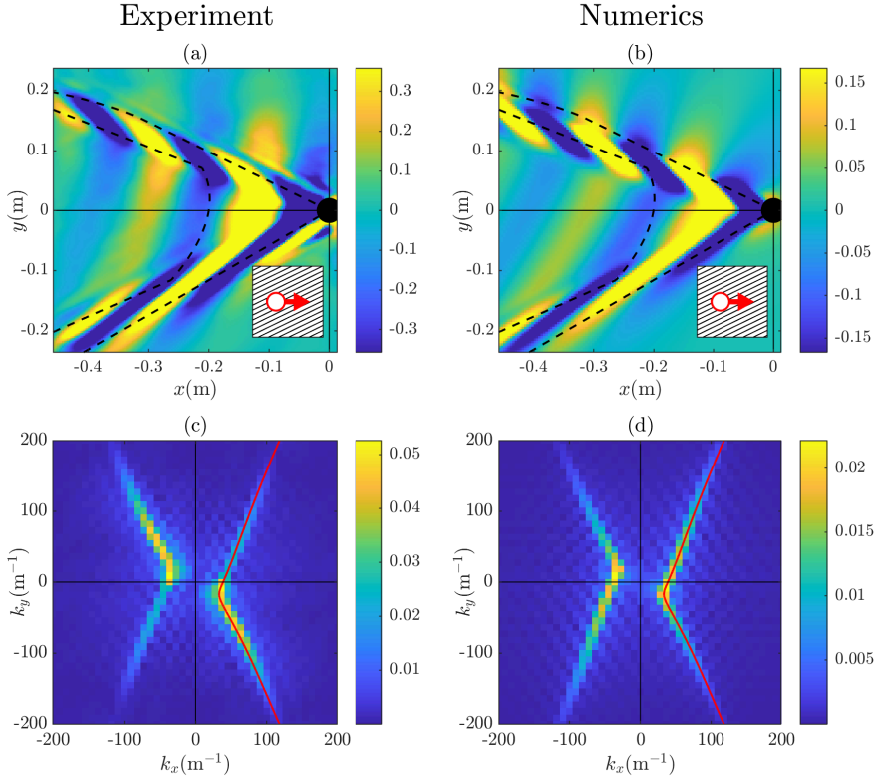


FIGURE 6. Surface elevation for the parameters $h^- = 10\text{mm}$, $h^+ = 55\text{mm}$, $h_X = 12\text{mm}$, $h_Y = 47.5\text{mm}$, $\alpha = -62^\circ$ and $U = 0.47\text{ms}^{-1}$. (a) Experimental results (colorscale in mm), the black dashed line indicated the schematic representation using the group velocity vectors (fig 3b), the inset shows the stratified bathymetry with the red arrow indicating the ship propagation. The color scale is saturated to emphasize the transverse waves. (c) Fourier transform of the experimental results, the red curve corresponds to the theoretical dispersion relation (2.2) and (2.3). (b) Numerical results (colorscale divided by the maximum value) and (d) its Fourier transform.

numerically investigated the effect of Hull Froude number on preferentially exciting long waves.

To get more quantitative comparison with theoretical aspects, we compute numerical results with Fourier transform technique (developed in Appendix A) for the same parameters as in the experiment. The good agreement between experimental and numerical results shows the validity of the anisotropic dispersion relation (2.3) and this is even clearer on the Fourier transform of the surface deformation (figure 5(c,d)). We can also observe that dissipation processes and non-linearities, which are not taken into account in the numerical computation, have no notable impact in the experimental results.

Another experiment is performed in a more symmetrical case. We measure a wake (figure 6) similar to the one with a Froude of less than 1 where the long waves are inside the apparent angle (figure 2(c)). For this case, we use the same bathymetry as before with an angle $\alpha = -62^\circ$ and a ship speed of $U = 0.47\text{m/s}$ (cross in figure 4). Due to the anisotropy, a remarkable effect is that the waves inside the apparent angle (transversal waves) are oblique. In the Fourier space (figure 6(c,d)), we see clearly the effect of the anisotropy on the dispersion relation.

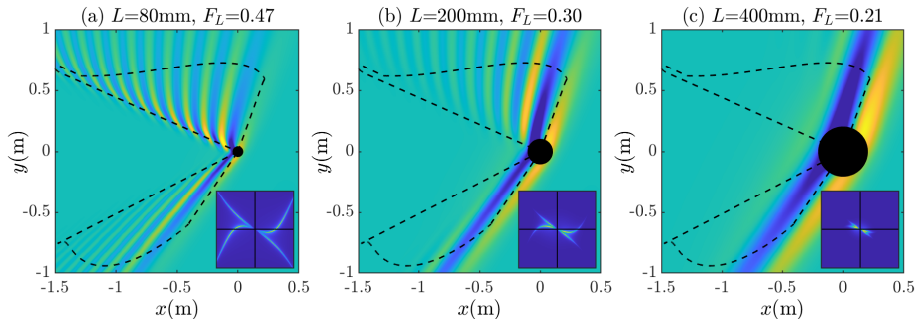


FIGURE 7. Numerical wakes (and its associated Fourier transform) on the stratified bathymetry with the parameters $h_X = 12\text{mm}$, $h_Y = 47.5\text{mm}$, $\alpha = -39^\circ$ and a ship speed $U = 0.42\text{ms}^{-1}$. The size of the ship L is varying from 80mm to 400mm (2 to 10 times the ship size in the experiments), with associated hull Froude number Fr^L from 0.47 to 0.21. The dashed curves indicates the schematic representation of the wake. The diameter of dotted circle on the right corresponds to the ship size in the Fourier space equal to $2/L$.

5. Hull Froude number and non-dispersive wake

In this section, we consider the evaluation of the effect of the ship size using numerical results, i.e. we will compute wakes with Fourier transform varying the Hull Froude number. Since long waves are more affected by the stratified bathymetry, we want to inspect if the size of the ship is able to enhance their role. To achieve this and to enhance long wave excitation, we need a bigger ship (thus a smaller hull Froude number $\text{Fr}^L = U/\sqrt{gL}$) and we use the numerical computation to observe wakes of a ship up to 10 times larger than the one used in the experiment.

Figure 7 shows wakes for the same parameters as the experimental results of figure 5 but with larger ship sizes. In the experiment $\text{Fr}^L \simeq 0.7$, and here we consider three different values of Fr^L ranging from 0.47 to 0.21 corresponding to boat sizes from 80mm to 400mm. We see that the amplitude of the short waves decreases as the size of the ship increases until only non-dispersive long waves remain. In figure 7(c), the wake appears simply as a Mach cone (or a Froude cone in our case) but with the peculiarity that the upper wake is completely ahead of the ship. In addition, it appears that is possible to control the shape of the Mach cone by properly choosing the bathymetry at low value of Fr^L . It is displayed in figure 8 for $\text{Fr}^L=0.17$ ($L = 600\text{mm}$) and for three different arrangements of bathymetry. From the classical Mach cone for flat bathymetry (figure 8(a)), through the asymmetrical cone in figure 8(b), we can construct a symmetric stratified bathymetry able to produce a surprising reversed cone where the wake entirely propagates in front of the ship. Incidentally, it can be noted in this figure that this behaviour is recovered by the classical geometrical way of constructing the Mach cone (developed in Appendix B).

6. Conclusion

We show, experimentally, theoretically and numerically, that a stratified bathymetry can generate highly asymmetrical wakes due to the anisotropy induced by the structured bottom. By construction, immersed structures do not affect the shorter wavelengths while long waves are able to present the strongest asymmetric behaviour. To design this asymmetry of the wake patterns, a simple two-dimensional effective medium model obtained from homogenization of the full three-dimensional water wave problem is used and is shown to accurately predict the experimental results. In addition to the asymmetry of the wake, it is observed that the bottom structuration can provoke long waves to

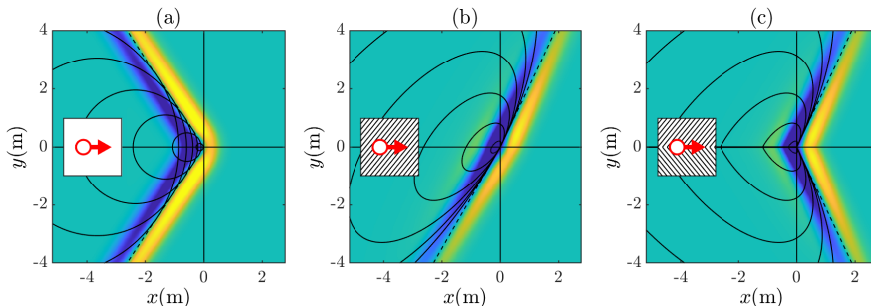


FIGURE 8. (a) Non-dispersive wake (due to a small hull Froude number $Fr^L = 0.17$) on a flat bathymetry with a water depth $h = h_X = 12\text{mm}$. The circles show the classical way to draw the Froude (Mach) cone. (b) Non-dispersive wake for the same parameter as figure 7 but with an hull Froude number $Fr^L = 0.17$. The ellipses draw the asymmetrical Froude cone. (c) Non-dispersive wake over a symmetrical bathymetry. The insets show the bathymetry with the red arrow indicating the ship propagation.

propagate ahead of the ship. The ability to modify ship wakes can have a significant impact on attenuating shoreline and riverbanks erosion as well as controlling wave resistance to reduce ship fuel consumption.

Funding

The authors acknowledge the support of the ANR under Grants No. ANR-21-CE30-0046 CoProMM.

Declaration of interests

The authors report no conflict of interest.

Author ORCIDs

L.-P. Euvé, <https://orcid.org/0009-0006-7757-643X>; A. Maurel, <https://orcid.org/0000-0001-8432-9871>; P. Petitjeans, <https://orcid.org/0000-0003-3179-0108> ; V. Pagneux, <https://orcid.org/0000-0003-2019-823X>.

Appendix A. Numerical Results

We consider that the pressure field of the ship (the ball) can be represented a source with a gaussian form : $F(x, y) = \exp(-(x^2 + y^2)/\sigma^2)$ with $\sigma = L/3$ (L the ship size). This value σ is fixed to obtain a good agreement between experimental and numerical results. In the Fourier space the source is given by : $F_k(k_x, k_y) = \exp(-(k_x^2 + k_y^2) \frac{1}{\sigma^2})$.

We obtain the surface elevation in the Fourier space thanks to the dispersion relation $\omega(k)$ and doppler effect :

$$\hat{\eta}(k_x, k_y) = \frac{F_k \omega^2}{k_x^2 U^2 - \omega^2 - 2i\epsilon k_x U - \epsilon^2} \quad (\text{A } 1)$$

with ϵ a small parameter controlling the attenuation to avoid aliasing. The wake in the real space is then obtained with an inverse Fourier transform of eq.(A 1).

Appendix B. Geometrical construction of Mach cone

Figure 8 shows the classical way of constructing the Froude cone. The circles correspond to a wave propagating in all directions at velocity c from time t and centered at $x = -Ut$ the position at the instant of emission in the ship referential. Superimposing these circles reveals the Froude cone with the known angle of $\sin(\beta) = c/U$ for a flat bathymetry as in figure 8(a) with $c = \sqrt{gh_X} = 0.34\text{ms}^{-1}$ and $U = 0.42\text{ms}^{-1}$. For the stratified bathymetry (figure 8(b)), we can use the same construction but, here, the velocity c depends on the direction resulting on ellipses which are solutions of $1 = X^2/c_X^2 + Y^2/c_Y^2$ with $c_X = \sqrt{gh_X} = 0.34\text{ms}^{-1}$ and $c_Y = \sqrt{gh_Y} = 0.68\text{ms}^{-1}$.

REFERENCES

- CAPLIER, C., ROUSSEAUX, G., CALLUAUD, D. & DAVID, L. 2016 Energy distribution in shallow water ship wakes from a spectral analysis of the wave field. *Physics of Fluids* **28** (10), 107104, arXiv: <https://pubs.aip.org/aip/pof/article-pdf/doi/10.1063/1.4964923/15855247/107104.1.online.pdf>.
- CAPLIER, C., ROUSSEAUX, G., CALLUAUD, D. & DAVID, L. 2020 Effects of finite water depth and lateral confinement on ships wakes and resistance. *J Hydrodyn* **32**.
- CARUSOTTO, I. & ROUSSEAUX, G. 2013 The Cerenkov Effect Revisited: From Swimming Ducks to Zero Modes in Gravitational Analogues | SpringerLink. In *Analogue Gravity Phenomenology, Lecture Notes in Physics*, vol. 870, pp. 109–144.
- DARMON, ALEXANDRE, BENZAQUEN, MICHAEL & RAPHAËL, ELIE 2014 Kelvin wake pattern at large froude numbers. *Journal of Fluid Mechanics* **738**, R3.
- ELLINGSEN, S. A 2014 Ship waves in the presence of uniform vorticity. *Journal of Fluid Mechanics* **742**.
- FANG, M. C., YANG, R. Y. & SHUGAN, I. V. 2011 Kelvin ship wake in the wind waves field and on the finite sea depth. *Journal of Mechanics* **27** (1), 71–77.
- HAVELOCK, TH 1909 The wave-making resistance of ships: a theoretical and practical analysis. *Proceedings of the Royal Society of London. Series A, Containing Papers of a Mathematical and Physical Character* **82** (554), 276–300.
- LI, Y. & ELLINGSEN, S. 2016 Ship waves on uniform shear current at finite depth: wave resistance and critical velocity. *Journal of Fluid Mechanics* **791**, 539–567.
- LUO, C., IBANESCU, M., JOHNSON, S.G. & JOANNOPOULOS, J. D. 2003 Cerenkov radiation in photonic crystals. *Science* **299** (5605), 368–371.
- MARANGOS, CHRISTOS & PORTER, RICHARD 2021 Shallow water theory for structured bathymetry. *Proceedings of the Royal Society A* **477** (2254), 20210421.
- MAUREL, A., MARIGO, J.-J., COBELLI, P., PETITJEANS, P. & PAGNEUX, V. 2017 Revisiting the anisotropy of metamaterials for water waves. *Physical Review B* **96** (13).
- MOISY, F. & RABAUD, M. 2014 Mach-like capillary-gravity wakes. *Physical Review E* **90** (2).
- MOISY, F., RABAUD, M. & SALSAC, K. 2009 A synthetic Schlieren method for the measurement of the topography of a liquid interface. *Experiments in Fluids* **46** (6), 1021.
- NOBLESSE, F., HE, J., ZHU, Y., HONG, L., ZHANG, C., ZHU, R. & YANG, C. 2014 Why can ship wakes appear narrower than Kelvin’s angle? *European Journal of Mechanics - B/Fluids* **46**, 164–171.
- PETHIYAGODA, R., MCCUE, S. W. & MORONEY, T. J. 2014 What is the apparent angle of a Kelvin ship wave pattern? *Journal of Fluid Mechanics* **758**, 468–485.
- PETHIYAGODA, R., MCCUE, S. W. & MORONEY, T. J. 2015 Wake angle for surface gravity waves on a finite depth fluid. *Physics of Fluids* **27** (6), 061701.
- RABAUD, M. & MOISY, F. 2013 Ship Wakes: Kelvin or Mach Angle? *Physical Review Letters* **110** (21), 214503.
- THOMSON, W. 1887 On Ship Waves. *Proceedings of the Institution of Mechanical Engineers* **38** (1), 409–434.